

# The Glycolytic Enzyme, GPI, Is a Functionally Conserved Modifier of Dopaminergic Neurodegeneration in Parkinson's Models

Adam L. Knight,<sup>1,5,6</sup> Xiaohui Yan,<sup>1</sup> Shusei Hamamichi,<sup>1</sup> Rami R. Ajjuri,<sup>1</sup> Joseph R. Mazzulli,<sup>3,8</sup> Mike W. Zhang,<sup>1</sup> J. Gavin Daigle,<sup>1,7</sup> Siyuan Zhang,<sup>1</sup> Akeem R. Borom,<sup>1</sup> Lindsay R. Roberts,<sup>1</sup> S. Kyle Lee,<sup>1</sup> Susan M. DeLeon,<sup>1</sup> Coralie Viollet-Djelassi,<sup>4</sup> Dimitri Krainc,<sup>3,8</sup> Janis M. O'Donnell,<sup>1</sup> Kim A. Caldwell,<sup>1,2</sup> and Guy A. Caldwell<sup>1,2,\*</sup>

<sup>1</sup>Department of Biological Sciences, The University of Alabama, Tuscaloosa, AL 35487, USA

<sup>2</sup>Departments of Neurology and Neurobiology, Center for Neurodegeneration and Experimental Therapeutics, Gregory Fleming James Cystic Fibrosis Research Center, University of Alabama at Birmingham, Birmingham, AL 35294, USA

<sup>3</sup>Department of Neurology, Massachusetts General Hospital, Harvard Medical School, MassGeneral Institute for Neurodegenerative Disease, Charlestown, MA 02129, USA

<sup>4</sup>Wellcome Trust Centre for Human Genetics, University of Oxford, Oxford OX3 7BN, UK

<sup>5</sup>The Babraham Institute, Cambridge CB22 3AT, UK

<sup>6</sup>Present Address: Synaptic Function Section, The Porter Neuroscience Research Center, National Institute of Neurological Disorders and Stroke, National Institutes of Health, Bethesda, MD 20892, USA

<sup>7</sup>Present Address: Department of Genetics, Louisiana State University Health Science Center, New Orleans, LA 70112, USA

<sup>8</sup>Present Address: The Ken and Ruth Davee Department of Neurology, Northwestern University Feinberg School of Medicine, Chicago IL 60611, USA

\*Correspondence: [gcaldwel@ua.edu](mailto:gcaldwel@ua.edu)

<http://dx.doi.org/10.1016/j.cmet.2014.04.017>

## SUMMARY

Neurodegenerative diseases represent an increasing burden in our aging society, yet the underlying metabolic factors influencing onset and progression remain poorly defined. The relationship between impaired IGF-1/insulin-like signaling (IIS) and life-span extension represents an opportunity to investigate the interface of metabolism with age-associated neurodegeneration. Using data sets of established DAF-2/IIS-signaling components in *Caenorhabditis elegans*, we conducted systematic RNAi screens in worms to select for *daf-2*-associated genetic modifiers of  $\alpha$ -synuclein misfolding and dopaminergic neurodegeneration, two clinical hallmarks of Parkinson's disease. An outcome of this strategy was the identification of GPI-1/GPI, an enzyme in glucose metabolism, as a *daf-2*-regulated modifier that acts independent of the downstream cytoprotective transcription factor DAF-16/FOXO to modulate neuroprotection. Subsequent mechanistic analyses using *Drosophila* and mouse primary neuron cultures further validated the conserved nature of GPI neuroprotection from  $\alpha$ -synuclein proteotoxicity. Collectively, these results support glucose metabolism as a conserved functional node at the intersection of proteostasis and neurodegeneration.

## INTRODUCTION

Parkinson's disease (PD) is an age-dependent neurodegenerative disease characterized by the accumulation of  $\alpha$ -synuclein

( $\alpha$ -syn) within Lewy bodies and the selective loss of dopamine (DA) neurons in the substantia nigra. While human genetic and genomic studies have illuminated various contributors to disease pathology, aging remains the single most definitive risk factor for the development of PD (Amaducci and Tesco, 1994). Therefore, an unresolved issue is the underlying molecular relationship between genetic factors influencing aging-associated metabolic changes and the loss of DA neurons associated with PD.

The IGF-1/insulin-like signaling (IIS) pathway has been implicated in human aging (Suh et al., 2008) and neurodegeneration (Cohen and Dillin, 2008). This pathway has been studied extensively in the nematode *Caenorhabditis elegans* (*C. elegans*), where mutation of DAF-2, the sole worm insulin/IGF-1 receptor, doubles lifespan and protects against a wide variety of cellular stressors. This effect is mediated through activation of DAF-16, the only FOXO/forkhead transcription factor (FOXO) in worms, which regulates the expression of numerous cytoprotective genes. In flies, reduced IIS via mutations in *chico*/insulin receptor substrate (IRS) extend lifespan and provide stress resistance (Clancy et al., 2001); phenotypes also are mediated by FOXO/FKHR (Yamamoto and Tatar, 2011). Similarly, mutations in *Drosophila* insulin-like receptor, the homolog of DAF-2, also extend lifespan in adult flies (Tatar et al., 2001). While the IIS pathway is comparably simplified in worms and flies, it is important to note that this signaling cascade is nearly identical to that in mammals (Taguchi and White, 2008). This provides the exciting opportunity to utilize age-modified animals to enrich for gene candidates involved in neurodegenerative disease processes.

Among proteotoxicity models in worms, reduced IIS has demonstrated protection against amyloid- $\beta$  (A $\beta$ ), polyglutamine-repeat (polyQ) proteins, and SOD-1 (Morley et al., 2002; Cohen et al., 2006; Boccitto et al., 2012). Similarly, expression of insulin-degrading enzyme in *Drosophila* suppresses A $\beta$  neurotoxicity (Tsuda et al., 2010). We previously established worm

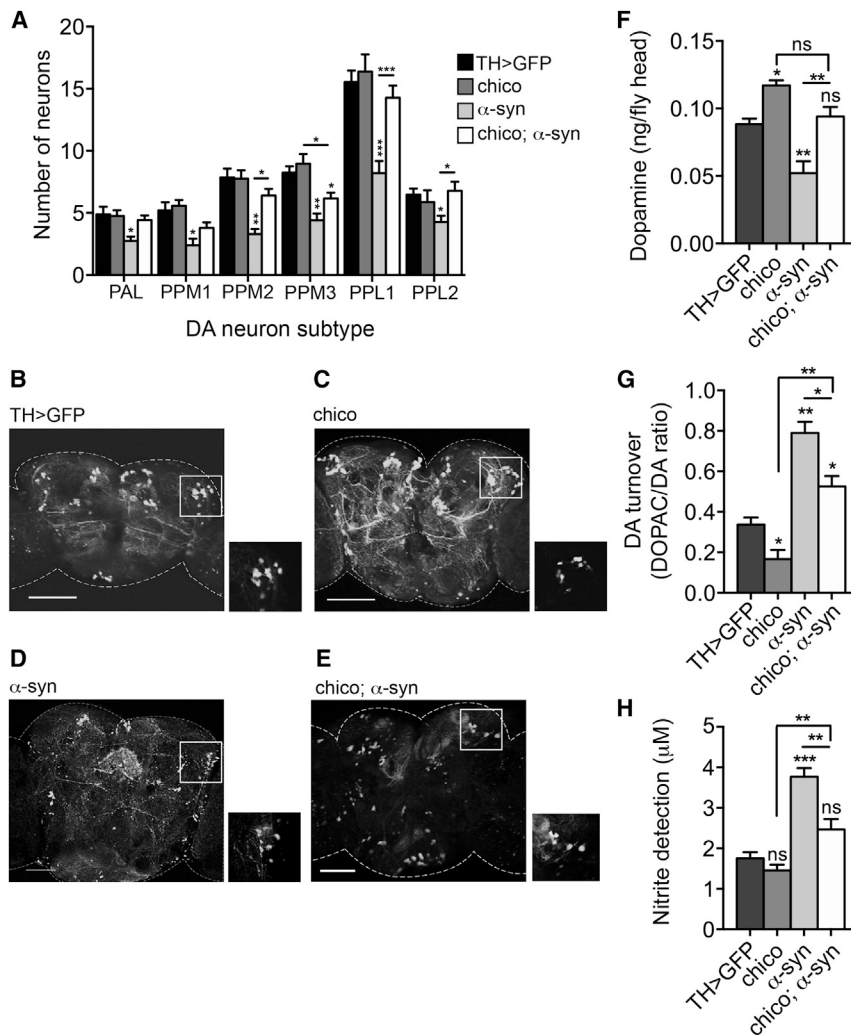


**Figure 1. *chico* Mutation Protects against Age-Dependent  $\alpha$ -syn Toxicity in DA Neurons**

DA neurons in the brains of 20-day-old adult males were visualized by expressing UAS-GFP tyrosine hydroxylase (TH)-Gal4.

(A) DA neurons were counted in each of the following DA subtype regions: anterior PAL (protocerebral anterolateral); posterior protocerebral posterior medial 1 (PPM1), PPM2, and PPM3; and posterior PPL1 and PPL2 (protocerebral posterolateral). Values are averages of 15 brains per genotype.

(B–E) Representative images of brains used for neuron counts with insets of the PPL1 region.

(F and G) DA and DOPAC pools in 20-day-old male heads. Values are averages of assays from three independent head extractions and three technical replicas for each extract, per genotype. Pools are quantified as ng per fly head.

(H) Nitric oxide synthase activity in brains of 20-day-old males was measured using a modified Griess Reagent assay. Results are displayed as  $\mu$ M concentration of nitrites in incubation medium. Values are averages of three replications of 20 fly brains per replication and three technical replicas per genotype. Genotypes tested were as follows: TH > GFP (UAS-GFP/+; TH-GAL4/+), *chico* (UAS-GFP/*chico*; TH-GAL4/+),  $\alpha$ -syn (UAS-GFP/+; TH-GAL4/UAS- $\alpha$ -syn), and *chico*;  $\alpha$ -syn (UAS-GFP/*chico*; TH-GAL4/UAS- $\alpha$ -syn). All values compared to TH > GFP controls unless otherwise indicated. \* $p$  < 0.05; \*\* $p$  < 0.01; \*\*\* $p$  < 0.001; one-way ANOVA with a Dunnett's post hoc test. Error bars indicate  $\pm$ SEM.

models in which two pathological hallmarks of PD,  $\alpha$ -syn-induced DA neurodegeneration (Cao et al., 2005) and  $\alpha$ -syn misfolding (Hamamichi et al., 2008), can be visualized and assayed. Similarly, we have established a *Drosophila* model for DA neurodegeneration, which takes advantage of its greater neuronal complexity to develop neurochemical and behavioral markers of PD-related degeneration (Chaudhuri et al., 2007). Here, we combine these established assay systems with the wealth of existing data on aging in these distinct models as a synergistic platform to uncover a relationship between metabolic change and neurodegeneration.

In this study, we report that reduced IIS suppresses  $\alpha$ -syn toxicity and DA neurodegeneration in *Drosophila* and *C. elegans*. We performed a large-scale RNAi screen in *C. elegans* to reveal 60 distinct genetic modifiers associated with this protection. Subsequent bioinformatic and functional analyses of these candidates identified GPI-1/GPI, a key enzyme in glucose metabolism, as a potent modifier of  $\alpha$ -syn misfolding and DA neurodegeneration in *C. elegans*. We also found that mutation of *Pgi*/GPI in *Drosophila* elevated a neuroinflammatory signal, disrupted DA homeostasis, and induced DA neurodegeneration. Lastly, this effect was translated to mammals, as *Gpi1*/GPI knockdown re-

sulted in  $\alpha$ -syn accumulation and neurotoxicity in mouse primary cortical neurons. These data from worms, flies, and mice collectively advance our understanding of proteotoxicity in the context of neurodegeneration, with glucose metabolism as a conserved unifying feature.

## RESULTS

### Reduced IIS Suppresses $\alpha$ -Syn-Induced DA Neurodegeneration in *Drosophila*

Although the IIS pathway is highly conserved in worms, flies, and mammals, a direct link between the IIS pathway and proteotoxicity or neurodegeneration has not previously been demonstrated in *Drosophila*. *Chico*/IRS mutations extend *Drosophila* lifespan and provide stress resistance (Clancy et al., 2001). To determine whether reduced IIS modulates  $\alpha$ -syn toxicity in flies, we evaluated DA neurons in the CNS of  $\alpha$ -syn-expressing adults heterozygous for a mutant *chico* allele. Quantification of these neuron clusters at day 1 (24–48 hr post-eclosion) revealed no significant variations in the number of DA neurons for any genotype (Figure S1A available online). At day 20, *chico* mutants maintain wild-type (WT) levels of DA neurons in all clusters (Figures 1A–1C). In contrast, flies expressing human  $\alpha$ -syn showed significant declines in neuron numbers in all DA neuron clusters. However, the presence of the *chico*

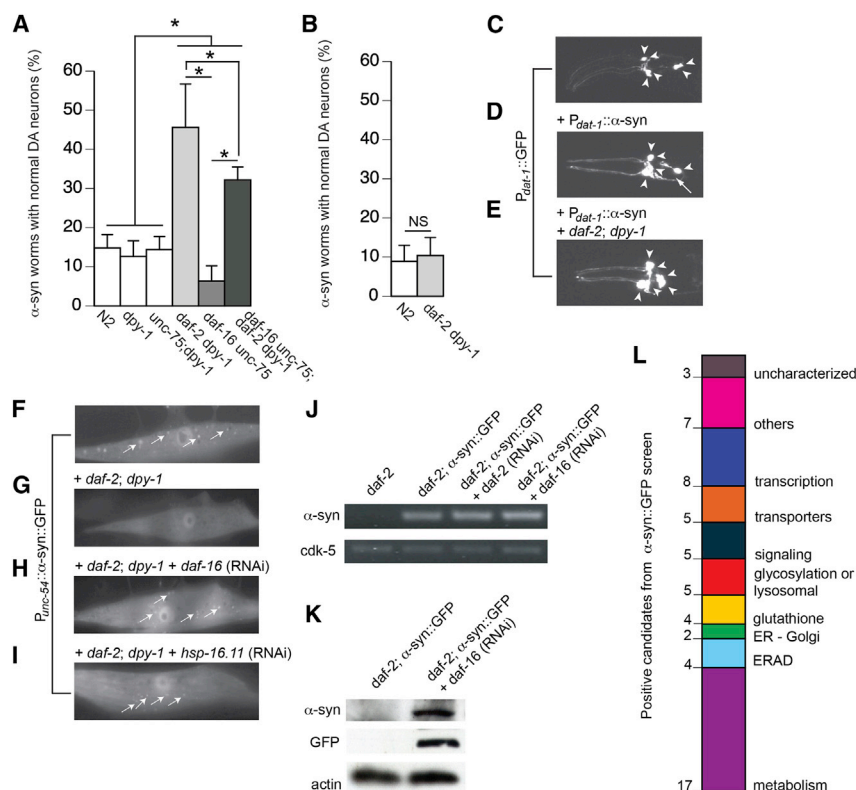


**Figure 2. IIS Pathway Modulates  $\alpha$ -Syn Aggregation and  $\alpha$ -Syn-Induced DA Neurodegeneration in *C. elegans***

(A–E) IIS pathway modulates  $\alpha$ -syn-induced DA neurodegeneration.

(A) IIS pathway modulates  $\alpha$ -syn-induced DA neurodegeneration at chronological aging (day 7) in worms. *daf-2* mutation dramatically suppressed  $\alpha$ -syn-induced DA neurodegeneration while the *daf-16* mutation enhanced  $\alpha$ -syn-induced DA neurodegeneration. Notably, the *daf-2; daf-16* double mutation moderately suppressed  $\alpha$ -syn-induced DA neurodegeneration at chronological aging. White bars indicate controls of the genetic backgrounds of the normal (N2), *daf-2*, and *daf-16* mutations.

(B) The *daf-2* mutation did not suppress  $\alpha$ -syn-induced DA neurodegeneration at biological aging (mean lifespan: day 20 for WT and day 40 for *daf-2* mutants). Three independent trials were performed ( $n = 90$  total), and positives were considered significant if  $p < 0.05$  via Student's *t* test.

(C–E) Representative images of DA neurons in *P<sub>dat-1</sub>::GFP* (C), *P<sub>dat-1</sub>::GFP + P<sub>dat-1</sub>:: $\alpha$ -syn* (D), and *P<sub>dat-1</sub>::GFP + P<sub>dat-1</sub>:: $\alpha$ -syn + *daf-2; dpy-1* mutant (E). Arrowheads denote normal neurons; arrows denote degenerated neurons.*

(F–L) IIS pathway modulates  $\alpha$ -syn aggregation.

(F) In the WT background,  $\alpha$ -syn::GFP accumulates in the cytoplasm of muscle cells.

(G) In the *daf-2* mutant background, the  $\alpha$ -syn::GFP fusion protein is completely degraded. This *daf-2* mutant +  $\alpha$ -syn::GFP strain was used in an RNAi screen.

(H and I) RNAi knockdown of *daf-16* and *hsp-16.11* resulted in a return of  $\alpha$ -syn::GFP aggregates in the *daf-2* background.

(J) Semiquantitative RT-PCR demonstrates that *daf-2* mutation and RNAi do not affect mRNA level of  $\alpha$ -syn::GFP.

(K) Western blot confirms the degradation of the fusion protein in the *daf-2* mutant background.

(L) Summary of the 60 positive candidates that, when knocked down by RNAi in a *daf-2* mutant +  $\alpha$ -syn::GFP strain, reproducibly enhanced  $\alpha$ -syn::GFP accumulation. Positive candidates were categorized using KOG and/or GO annotations.

Error bars indicate  $\pm$ SD.

mutation suppressed  $\alpha$ -syn-induced DA neuron loss (Figures 1A–1E).

### IIS Mediates DA Homeostasis and Inflammatory Signaling in *Drosophila*

To investigate the effect of *chico* on DA homeostasis, we quantified cellular DA levels and turnover. At day 1,  $\alpha$ -syn flies showed no significant change in DA pools relative to the WT control (Figure S1B). Interestingly, *chico* mutant flies and *chico* mutant- $\alpha$ -syn flies exhibited elevated levels of DA when compared to either WT or  $\alpha$ -syn flies alone (Figure S1B). By day 20, all genotypes except  $\alpha$ -syn have experienced a slight, age-dependent reduction in DA (compare Figures 1F and S1B), while the  $\alpha$ -syn flies displayed strongly reduced DA, relative to controls. *chico* mutation rescued the effect of  $\alpha$ -syn on DA (Figure 1F).

We then quantified the ratio of DOPAC:DA, which we have shown to be elevated in *Drosophila* DA neurons prior to degeneration (Chaudhuri et al., 2007). Analysis of 1-day-old flies revealed no significant change in DA turnover in *chico* or *chico;  $\alpha$ -syn* versus the control, but elevated DA turnover was evident in  $\alpha$ -syn flies (Figure S1C). At 20 days posteclosion, control flies had a slight increase in DA turnover associated with normal aging, while *chico* mutants remained virtually unchanged (Figure 1G). Thus, flies expressing  $\alpha$ -syn exhibit elevated DA

turnover, which is partially rescued in the *chico;  $\alpha$ -syn* strain (Figure 1G).

We tested whether there was an accompanying inflammatory response associated with these phenotypes. Using a modified Griess reagent assay (Ajuri and O'Donnell, 2013), we determined the levels of secreted nitrites, a stable metabolite of NO, as a measure of relative inflammatory response. At day 1,  $\alpha$ -syn flies displayed an increase in NO levels, while *chico* and *chico;  $\alpha$ -syn* showed little variation from controls (Figure S1D). A strong increase in NO levels was observed in  $\alpha$ -syn flies after 20 days of aging, which was significantly reduced in *chico;  $\alpha$ -syn* transgenic flies (Figure 1H). Taken together, these findings suggest the *Drosophila* IIS pathway can influence  $\alpha$ -syn-induced DA neurotoxicity.

### IIS Pathway Modulates $\alpha$ -Syn-Induced DA Neurodegeneration in *C. elegans*

Next, we investigated whether the link between the IIS pathway and  $\alpha$ -syn toxicity represents an evolutionarily conserved mechanism that may be applicable toward understanding PD. We performed genetic crosses to generate *daf-2* mutant worms that overexpress human  $\alpha$ -syn and GFP in DA neurons. At day 7, we found that only 15% of  $\alpha$ -syn worms displayed the WT complement of six anterior DA neurons (Figures 2A and 2D)

compared to worms expressing GFP alone, which have 100% WT DA neurons (Figure 2C) (Hamamichi et al., 2008). Strikingly, 40% of *daf-2*;  $\alpha$ -syn worms exhibited complete retention of DA neurons (Figures 2A and 2E). A well-characterized downstream component of the IIS pathway is DAF-16/FOXO, which functions as a key regulator of numerous cytoprotective genes (Murphy et al., 2003). We examined *daf-16* mutants that overexpress  $\alpha$ -syn + GFP in DA neurons. As predicted, *daf-16* mutation enhanced neurodegeneration (Figure 2A). Surprisingly, we observed an intermediate level of neuroprotection in *daf-2*; *daf-16* double mutants overexpressing  $\alpha$ -syn + GFP in DA neurons (Figure 2A). We verified that the genetic markers (*unc-75* and *dpy-1*) used in these mutants did not affect the DA neurodegeneration phenotype by examining the balancers alone (Figure 2A) and by crossing  $\alpha$ -syn into the same *daf-2* and *daf-16* alleles balanced with different genetic markers (Figure S2A). Our findings that *daf-2* mutation dramatically suppressed neurodegeneration, *daf-16* mutants enhanced neurodegeneration, and *daf-2*; *daf-16* double mutants suppressed neurodegeneration (although not to the same extent as *daf-2* mutants) indicate that DAF-16 is not the only genetic component responsible for DA neuroprotection. Additional pathways downstream of DAF-2 must contribute to neuroprotection.

### DA Neurodegeneration at Biological versus Chronological Aging in Worms

Associated with *daf-2* mutant lifespan extension is a delayed rate of aging. We questioned whether *daf-2*-mediated neuroprotection at day 7 (chronological aging) might result from slower development than WT (N2) control animals. We performed lifespan assays to determine biological aging (mean lifespan) and found that it was 20 days for WT; $\alpha$ -syn worms while it was 40 days for *daf-2*;  $\alpha$ -syn worms (data not shown). Interestingly, we found that *daf-2* was no longer neuroprotective at biological aging (Figures 2B and S2B). These findings, together with our results demonstrating IIS-mediated neuroprotection at chronological aging in worms (Figures 2A and S2A) and flies (Figure 1), suggest that the metabolic changes associated with reduced IIS are responsible for protection against  $\alpha$ -syn proteotoxicity and DA neurodegeneration.

### RNAi Screen for IIS-Mediated Protection against $\alpha$ -Syn Misfolding

We next sought to identify the genetic factors responsible for this IIS pathway-mediated protection against  $\alpha$ -syn by generating a *daf-2* strain that overexpresses  $\alpha$ -syn::GFP in muscle cells. Misfolded  $\alpha$ -syn::GFP fusion protein accumulated in the cytoplasm of N2 worms (Figure 2F), while in *daf-2* mutants the fusion protein was almost undetectable (Figure 2G). We reasoned that *daf-2* mutation likely promoted degradation of the fusion protein rather than affecting the  $\alpha$ -syn::GFP expression level (Figures 2J and 2K). We then knocked down *daf-16* and *hsp-16.11* (positive controls) via RNAi in *daf-2*;  $\alpha$ -syn::GFP worms and discovered that GFP inclusions reproducibly returned in these animals (Figures 2H and 2I).

To conduct the RNAi screen, we compiled a list of candidate genes and/or proteins with clear human orthologs that are upregulated in the *daf-2* background (Murphy et al., 2003; McElwee et al., 2004; Halaschek-Wiener et al., 2005; Dong et al., 2007)

and genes that mediate *daf-2* lifespan extension (Samuelson et al., 2007). We included genes upregulated upon pan-neuronal overexpression of  $\alpha$ -syn (Vartiainen et al., 2006) and previously identified genetic modifiers of  $\alpha$ -syn misfolding and toxicity in worms (Hamamichi et al., 2008; Kuwahara et al., 2008; van Ham et al., 2008). In total, we assayed 625 targets in triplicate and identified 60 genes that, when knocked down by RNAi, reproducibly enhanced  $\alpha$ -syn::GFP accumulation in the *daf-2* mutant background (Tables S1 and S2; Figure 3A). These positive hits were categorized into functional groups using KOG and GO annotations (Figure 2L; Table S2).

### Examination of IIS-Mediated $\alpha$ -Syn Modifiers in Additional Proteostasis Models

We next determined whether the 60 candidates were specific to  $\alpha$ -syn misfolding or are more general effectors of proteostasis. A previous study identified genetic modifiers of polyQ aggregation (Nollen et al., 2004), but none of those reported were identified in the *daf-2* background. We generated *daf-2* worms that overexpress Q82::GFP in muscle cells and, consistent with a previous report (Morley et al., 2002), found that reduced IIS suppressed polyQ aggregation (Figures 3B and 3C). We then performed RNAi of the 60 candidates to identify genes that, when knocked down in the *daf-2* + Q82::GFP background, enhanced polyQ aggregation (Figures 3A–3E). We discovered that 11/60 modifiers of  $\alpha$ -syn misfolding also affected polyQ aggregation (Figure 3F; Table S2).

We further investigated whether any of the 60 candidates modified amyloid-beta (A $\beta$ ) peptide toxicity. To evaluate these targets, an established worm model that utilizes temperature-sensitive induction of A $\beta$ -induced paralysis (Dostal and Link, 2010) was employed. We found that 8/60 targets enhanced A $\beta$ -induced paralysis (Figures S3A and S3B; Table S2).

In total, we found that 18/60  $\alpha$ -syn effectors also modified polyQ or A $\beta$  misfolding; one gene (Y45F10B.9, an uncharacterized zinc-finger protein) impacted misfolding in all three models. Thus, many of these genes appear to be general age-associated modifiers of proteostasis that may affect susceptibility to a variety of protein misfolding diseases.

### The Majority of $\alpha$ -Syn Modifiers Act Independent of DAF-16/FOXO

Since DAF-16 is a key regulator of numerous cytoprotective genes and was found to mediate  $\alpha$ -syn misfolding (Figure 2H) and DA neurodegeneration (Figure 2A), we investigated whether the 60 identified effectors were DAF-16 dependent. We performed genetic crosses to generate *daf-2*; DAF-16::GFP worms to visualize the distribution of DAF-16 within cells. Consistent with previous reports (Lin et al., 2001), we observed predominantly nuclear localization of DAF-16 in untreated and empty vector (EV) control RNAi-fed animals and increased cytoplasmic distribution of DAF-16 in *daf-18* RNAi-fed animals, in accordance with *daf-18* negative regulation of DAF-16 activity (Figure 3G–3I). We performed RNAi against each of the 60 targets and examined the knockdown effect on DAF-16 localization. Surprisingly, we found that only 11/60 candidates altered the distribution of DAF-16 within worms, including 3/17 metabolism-categorized candidates (Figures 3A and 3J; Table S2). For example, a metabolic candidate, *gpi-1*, when knocked

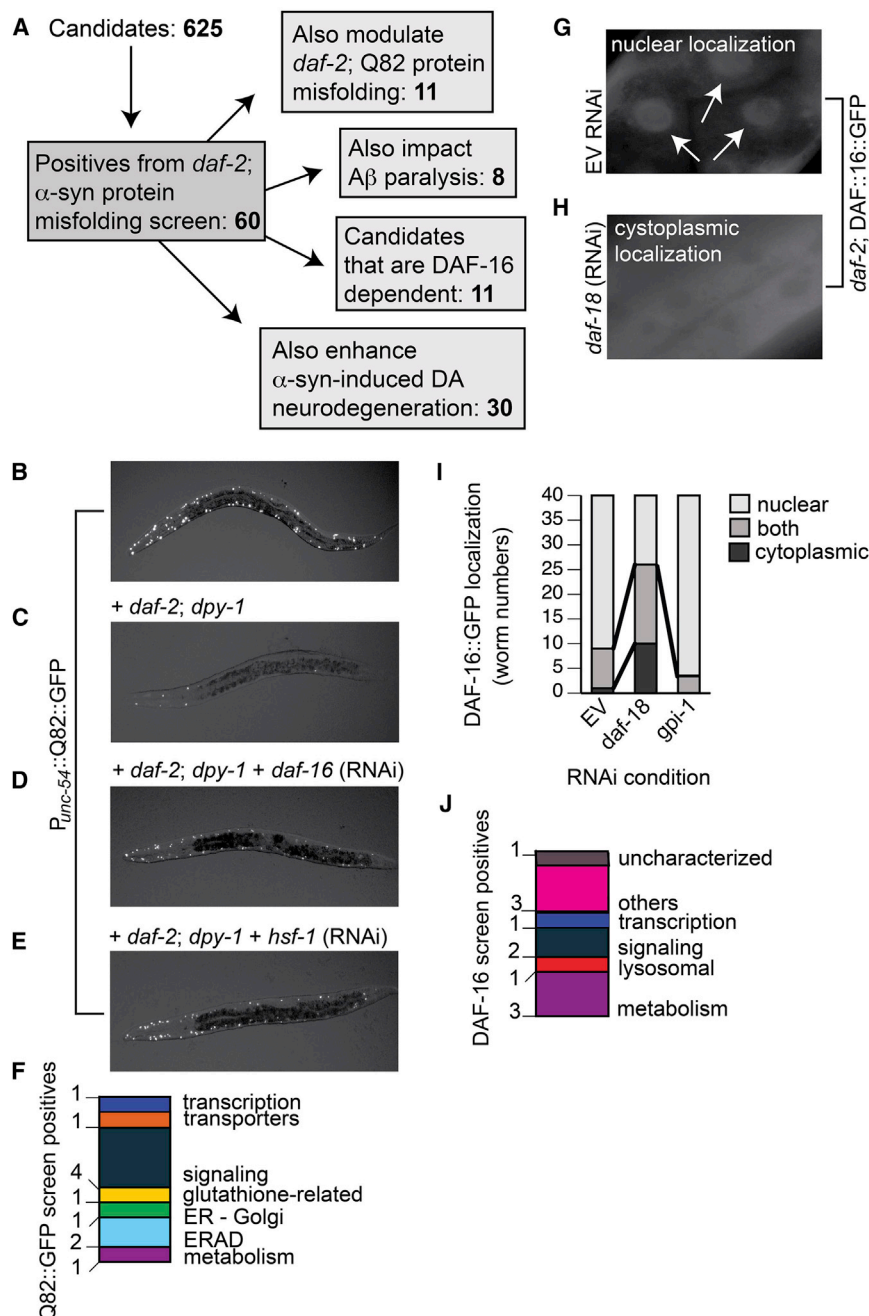


**Figure 3. Secondary Screening of Positive Candidates**

(A) Summary of secondary RNAi screens. (B) In the WT background, Q82::GFP accumulates in the cytoplasm of muscle cells. (C) Q82::GFP aggregation is suppressed in *daf-2* mutants, with approximately  $9 \pm 2$  aggregates per worm. (D and E) RNAi knockdown of *daf-16* or *hsf-1* in *daf-2* mutant background caused a return of the formation of Q82::GFP aggregates, with averages of  $18 \pm 1$  and  $23 \pm 6$  aggregates per worm, on average. We used the *daf-2* + Q82::GFP worms (C) to screen for modifiers of polyglutamine aggregation. (F) Summary of the candidates that, when knocked down in *daf-2* mutant background, significantly enhanced polyQ aggregation. Two independent trials ( $n = 40$  total) were performed, and positives were determined as significant if  $p < 0.05$ ; one-way ANOVA with Dunnett post hoc test. (G) In *daf-2* mutants treated with EV control RNAi, DAF-16::GFP is localized to the nucleus (arrowheads). (H) In *daf-2* mutants treated with *daf-18* RNAi, DAF-16::GFP is distributed evenly throughout the cytoplasm. (I) Graph showing quantification of DAF-16::GFP localization in worms. Localization was scored as “nuclear” (light gray), “cytoplasmic” (black), or “both” nuclear and cytoplasmic (dark gray). In *daf-2* mutants fed EV RNAi, DAF-16::GFP is predominantly localized to the nucleus. In *daf-2* mutants exposed to the RNAi clone targeting *daf-18* there is increased cytoplasmic distribution of DAF-16::GFP. We performed RNAi against all 60 positive candidates in *daf-2*; DAF-16::GFP worms and examined the effect of candidate knockdown on DAF-16 localization versus the DAF-16::GFP pattern obtained with mock, or EV, RNAi knockdown. One candidate from our screen, *gpi-1* (RNAi), is displayed in this graph. (J) Summary of candidates that, when knocked down, altered DAF-16::GFP localization. Two independent trials ( $n = 40$  total) were performed, and positives were determined as significant if  $p < 0.05$  via chi-square test.

down, did not have an overt effect on DAF-16::GFP localization in the *daf-2* background (Figure 3I; Table S2). Thus, while some candidates may function as DAF-16-dependent effectors of  $\alpha$ -syn misfolding, the majority of these modifiers appear to modulate proteotoxicity through distinct mechanisms.

In order to further define mechanistic pathways that may be enriched in our screens, we analyzed our 60  $\alpha$ -syn modifiers using IPA, which relies on the Ingenuity Pathway Knowledge Base. Table S3 shows the five most significant functional networks of  $\alpha$ -syn modifiers identified by IPA analysis. The leading network included functional categories of energy production and nucleic acid metabolism. We further investigated the most

21 proteins from our initial 60  $\alpha$ -syn modifiers interact within this network, revealing an important role for metabolism in age-associated  $\alpha$ -syn toxicity. We hypothesize this subset of functional modifiers mediate metabolic changes connected to PD.

### Examination of IIS-Mediated $\alpha$ -Syn Modifiers in *C. elegans* DA Neurons

Next we assessed whether our 60 candidate genes modify  $\alpha$ -syn-induced DA neurodegeneration independent of the *daf-2* mutation. Our reasoning was 2-fold: (1) most candidates were not *daf-16* dependent, and (2) as described in Figure 2A, *daf-2*;

significant functional network by visualizing its interaction with *daf-2*/IGFR and *daf-16*/FOXO (Figure S4). We found that

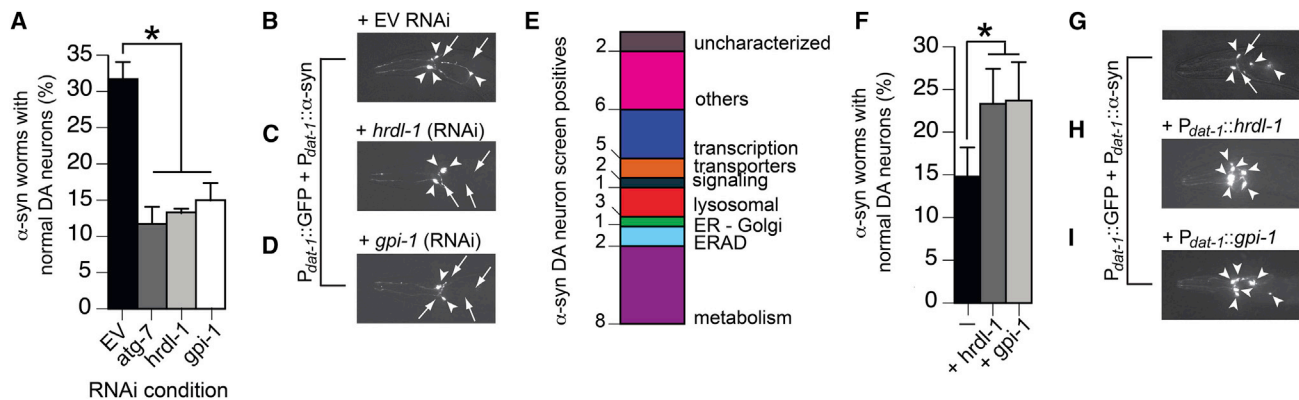


**Figure 4. IIS-Associated Modifiers of  $\alpha$ -Syn Misfolding Also Affect  $\alpha$ -Syn-Induced DA Neurodegeneration**

(A) Graph showing percentage of 6-day-old worms with normal DA neurons for two RNAi targeting controls (EV and *atg-7*) and two positive candidates from RNAi screen (*gpi-1* and *hrdl-1*). RNAi targeting each of the 60 candidates was performed in *sid-1* mutant worms overexpressing *P<sub>unc-119</sub>::sid-1* + *P<sub>dat-1</sub>::GFP* + *P<sub>dat-1</sub>::α-syn*.

(B–D) Representative images of *P<sub>unc-119</sub>::SID-1* + *P<sub>dat-1</sub>::GFP* + *P<sub>dat-1</sub>::α-syn* worms treated with EV RNAi (B), *hrdl-1* RNAi (C), and *gpi-1* RNAi (D). Arrowheads show intact DA neuron cell bodies. Arrows indicate areas where DA neurons have degenerated.

(E) Summary of candidates that, when knocked down, enhanced DA neurodegeneration in transgenic worms expressing *P<sub>unc-119</sub>::sid-1* + *P<sub>dat-1</sub>::GFP* + *P<sub>dat-1</sub>::α-syn*.

(F) Graph showing the percentage of 7-day-old worms with normal DA neurons for *P<sub>dat-1</sub>::GFP* + *P<sub>dat-1</sub>::α-syn* worms overexpressing either *hrdl-1* or *gpi-1*.

(G–I) Representative images of *P<sub>dat-1</sub>::GFP* + *P<sub>dat-1</sub>::α-syn* worms (G), *P<sub>dat-1</sub>::GFP* + *P<sub>dat-1</sub>::α-syn* + *P<sub>dat-1</sub>::hrdl-1* worms (H), and *P<sub>dat-1</sub>::GFP* + *P<sub>dat-1</sub>::α-syn* + *P<sub>dat-1</sub>::gpi-1* (I). \**p* < 0.05, one-way ANOVA with Dunnett post hoc test. Error bars indicate  $\pm$ SD.

*daf-16* double mutants only decrease  $\alpha$ -syn-induced DA neurodegeneration by 13%, compared to a 30% decrease in the WT background, suggesting there are additional pathways impacting neuroprotection in parallel to DAF-16. We utilized a worm strain that enables DA neuron-selective RNAi with transgenic animals expressing  $\alpha$ -syn (and GFP) in DA neurons to knock down the 60 IIS-related candidates (Harrington et al., 2012). We found that 30/60 candidates upon RNAi treatment significantly enhanced DA neurodegeneration (Figure 4A–4E; Table S2). Interestingly, 10/30 positives were involved in the energy production and metabolism IPA network (Figure S3), including glucose-6-phosphate isomerase (*gpi-1*/GPI), a key enzyme in glycolysis. Interestingly, when GPI-1 is secreted by cancer cells, it can also serve as a cytokine to activate autocrine motility factor (AMF) signaling (Haga et al., 2000). It was therefore significant that the receptor for AMF (*hrdl-1*/AMFR) was also identified in this screen. Accordingly, both *gpi-1* and *hrdl-1* RNAi enhanced  $\alpha$ -syn-induced DA neurotoxicity (Figures 2L and 4A–4D; Table S2). Conversely, overexpression of *gpi-1* and *hrdl-1* in DA neurons resulted in significant protection from  $\alpha$ -syn-induced neurotoxicity (Figures 4F–4I).

#### GPI-1 Protects DA Neurons in Parallel to DAF-16

To investigate the mechanism for GPI-1-mediated neuroprotection, we performed combinatorial RNAi against *daf-2* + *gpi-1* and *daf-2* + *hrdl-1* to determine whether *daf-2*-mediated neuroprotection is dependent on these gene products. Combinatorial RNAi eliminated the neuroprotection phenotype conferred by *daf-2* RNAi (Figure 5A). Notably, neuroprotection decreased 79% in *daf-2*; *gpi-1* double RNAi versus 30% in *daf-2*; *daf-16* double mutants (Figures 5A versus 2A), suggesting the cellular events involving *gpi-1* provide greater protection than the DAF-16 pathway. We also found that combinatorial RNAi against

*daf-16* + *gpi-1* enhances DA neurodegeneration compared to *gpi-1* RNAi alone (Figure 5B), providing further evidence that *gpi-1* is functioning independently of *daf-16*. We validated this result with quantitative RT-PCR and found that *gpi-1* RNAi did not significantly impact the expression level of two known endogenous DAF-16 transcriptional targets, *sod-3* and *mtl-1* (Robida-Stubbs et al., 2012). Similar results were observed in the WT genetic background (Figure 5C).

#### GPI-1 Influences Protein Homeostasis through Glycolysis

We tested whether GPI-1 could regulate the folding of endogenous metastable proteins by using worm strains carrying temperature-sensitive (*ts*) mutations *unc-15(e1402)* and *unc-52(e669su250)*, encoding paramyosin and perlecan, respectively. At permissive temperature, these *ts* metastable proteins fold and function properly, while at elevated temperature the proteins misfold and induce motility defects (Gidalevitz et al., 2006). Figure 5D shows that *gpi-1* RNAi at permissive temperature significantly (*p* < 0.01) reduced the motility of young adult *unc-15* and *unc-52* worms by 46% and 37%, respectively, suggesting a role for GPI-1 in maintaining global proteostasis.

To study the underlying mechanism impacting proteostasis, we inquired whether GPI-1 neuroprotection involved glycolysis, since this enzyme is involved in its initial steps. Treatment with 2-deoxyglucose (DOG), a glucose analog that blocks glycolysis, enhanced  $\alpha$ -syn-induced DA neurodegeneration in worms (Figure 5E) and  $\alpha$ -syn-induced motility defects in flies (Figure 5F). Importantly, combinatorial treatment of worms with DOG + *gpi-1* RNAi did not enhance  $\alpha$ -syn-induced DA neurodegeneration compared to *gpi-1* RNAi alone (Figure 5E). In addition, excess glucose suppressed  $\alpha$ -syn-induced motility defects in *Drosophila* (Figure 5F; Movies S1, S2, and S3). Lastly, we

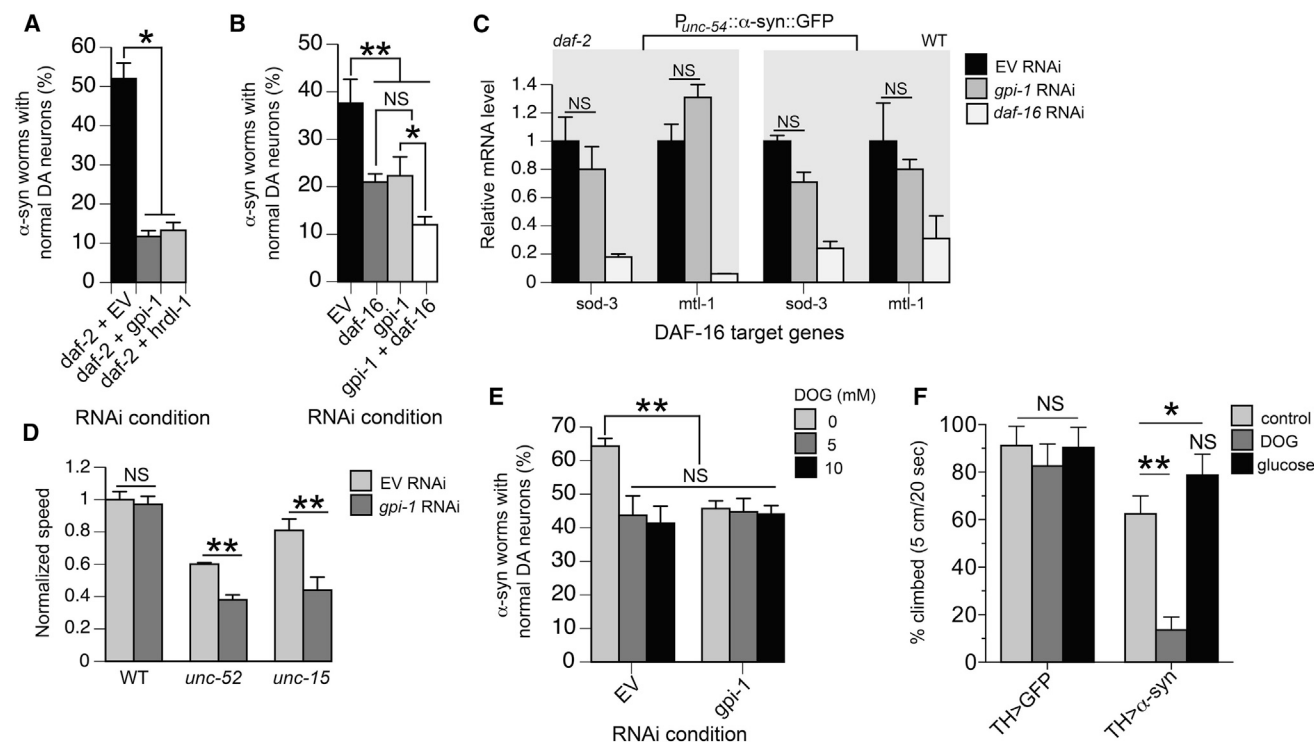


**Figure 5. GPI-1 Mechanistic Analyses**

(A and B) Graphs depicting percentage of 6-day-old worms with normal neurons following combinatorial RNAi of *daf-2* + EV control, *gpi-1*, or *hrdl-1* (A) and combinatorial RNAi of *daf-16* + EV control or *gpi-1* (B) in *P<sub>unc-119</sub>::sid-1* + *P<sub>daf-1</sub>::GFP* + *P<sub>daf-1</sub>:: $\alpha$ -syn* *C. elegans*. \**p* < 0.05; \*\**p* < 0.01, one-way ANOVA with Dunnett post hoc test.

(C) No induction of endogenous DAF-16 target genes in response to *gpi-1* RNAi. Quantitative RT-PCR was performed with young adult *daf-2* mutant or N2 WT worms expressing *P<sub>unc-54</sub>:: $\alpha$ -syn::GFP*, treated with EV control RNAi, *gpi-1* RNAi, or *daf-16* RNAi (positive control). For each *daf-16* target gene, its mRNA levels were normalized to the expression in worms treated with EV control RNAi. Values are means  $\pm$ SD (*n* = 3 independent biological samples with 100 worms in each). *P* value was calculated by nonparametric one-way ANOVA. NS, not significant, compared with worms treated with EV control RNAi.

(D) *gpi-1* RNAi at permissive temperature (16°C throughout the experiment) significantly reduced the motility of young adult *unc-15*(*e1402*) and *unc-52*(*e669su250*) worms. Animals were exposed to EV or *gpi-1* RNAi from embryos. The movement of young adult worms were recorded and analyzed by WormLab3.0 with the crawling mode. Values are means  $\pm$ SD (*n* = 3 independent experiments with 15–20 worms in each). \*\**p* < 0.01, unpaired Student's two tailed *t* test with Welch correction.

(E) Graph showing percentage of 4-day-old worms with normal DA neurons. *P<sub>unc-119</sub>::sid-1* + *P<sub>daf-1</sub>::GFP* + *P<sub>daf-1</sub>:: $\alpha$ -syn* worms fed EV control RNAi or *gpi-1* RNAi were treated with 0 mM, 5 mM, and 10 mM 2-DOG and then analyzed 24 hr after exposure. \*\**p* < 0.01, one-way ANOVA with Dunnett post hoc test. For (A)–(E), error bars indicate  $\pm$ SD.

(F) Mobility of  $\alpha$ -syn expressing flies aged to 10 days and then fed 200 mM DOG or 1 M glucose for 5 days. \**p* < 0.05; \*\**p* < 0.01, one-way ANOVA with Bonferroni post hoc test. Error bars indicate  $\pm$ SEM.

quantified ATP levels in worms treated with *gpi-1* RNAi and found these were unaffected (Figure S5), implying certain glycolytic metabolites may be responsible neuroprotection. Along with prior studies (Schulz et al., 2007; Tauffenberger et al., 2012), these data provide strong evidence that GPI-1 mediates proteotoxicity via glycolysis.

### Pgi/GPI Mutation Induces DA Neurodegeneration in *Drosophila*

We sought to investigate whether a relationship between glucose metabolism, proteostasis, and neurodegeneration is conserved in other species. To this end, we first examined the link between IIS and the *gpi-1* fly ortholog *pgi*. While heterozygous *chico* mutants had no deficiency in climbing behavior, heterozygous *pgi* mutants displayed a significant reduction in mobility relative to WT flies (Figure 6A). The presence of the

mutant allele of *chico* in double heterozygotes was unable to rescue the climbing deficits of heterozygous *pgi* mutants. This result suggests that *pgi* acts downstream of *chico* or that the two genes function in genetically separate pathways.

Next we examined whether *pgi* modulates  $\alpha$ -syn-induced DA neurodegeneration. A heterozygous *pgi* mutation was introduced into flies expressing  $\alpha$ -syn and GFP in DA neurons, under the control of a *TH-GAL4* driver. To investigate the effect of *pgi* on  $\alpha$ -syn toxicity, we compared DA neuron numbers for the WT and heterozygous *pgi* mutant genotypes in GFP-expressing neurons, in the absence and presence of  $\alpha$ -syn. No significant changes were observed DA neuron numbers for any genotype at day 1 posteclosion (Figure S6A). However, we found a significant decline at day 20 in DA neuron numbers in *pgi* heterozygous mutant brains in the absence of  $\alpha$ -syn (Figures 6B–6D). Similarly,  $\alpha$ -syn, *pgi*<sup>WT</sup> flies exhibited significant degeneration

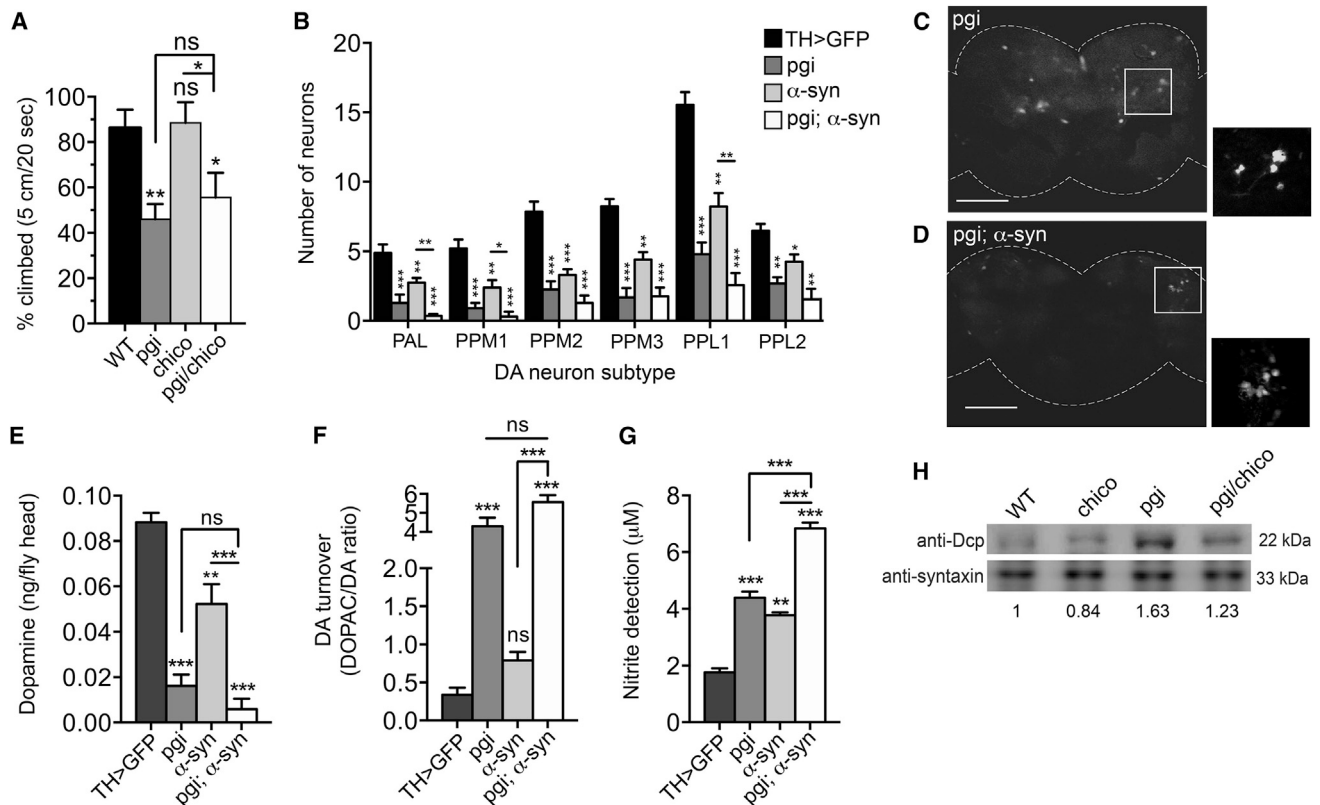


**Figure 6. *Pgi*/GPI Mutation Enhances  $\alpha$ -Syn-Induced DA Neuron Loss**

(A) Mobility assays of heterozygous *chico* and *pgi* mutant alleles, individually and in combination, relative to WT flies. (B–D) DA neurons in the brains of 20-day-old adult males, visualized by TH-Gal4 driven GFP. (B) Neurons were counted in anterior and posterior DA neuron clusters. Values are averages of 15 brains per genotype. (C and D) Representative images of brains used for neuron counts with insets of the PPL1 region. (E and F) DA and DOPAC pools were measured in heads of 20-day-old male flies. Assay values were determined using three independent head extracts and three technical replicas for each genotype and calculated as ng per fly head. (G) Nitric oxide synthase activity in brains of 20-day-old males was measured using a modified Griess Reagent assay. Results are displayed as  $\mu$ M concentration of nitrites in incubation medium. Values are averages of three replications of 20 fly brains per replication and three technical replicas per genotype. Genotypes for strains tested are as follows: TH > GFP (*UAS-GFP/+*; *TH-GAL4/+*), *Pgi* (*UAS-GFP/Pgi*; *TH-GAL4/+*),  $\alpha$ -syn (*UAS-GFP/+*; *TH-GAL4/UAS- $\alpha$ -syn*), and *Pgi;  $\alpha$ -syn* (*UAS-GFP/Pgi*; *TH-GAL4/UAS- $\alpha$ -syn*). These assays were performed simultaneously with those in Figure 1 and employed the same TH>GFP controls. \* $p < 0.05$ ; \*\* $p < 0.01$ ; \*\*\* $p < 0.001$ ; one-way ANOVA followed by Dunnett's post hoc test analysis. Error bars indicate  $\pm$ SEM. (H) Western blot reveals that levels of the apoptosis factor *death caspase-1* (DCP-1) in 20-day-old adult male heads was elevated 1.6-fold in the *pgi* mutant flies and reduced slightly in *chico* alone (0.83:1). Expression of *chico* and *pgi* together only slightly ameliorated DCP-1 protein expression relative to WT (1.23:1).

of DA neurons (Figure 6B). The combination of the *pgi* mutant allele with  $\alpha$ -syn significantly reduced neuron numbers further in nearly all DA neuron clusters (Figures 6B–6D).

#### Pgi/GPI Mutation Exacerbates the Effects of $\alpha$ -Syn on DA Metabolism and Nitric Oxide Production in *Drosophila*

Since glucose restriction increases oxidative stress in worms (Schulz et al., 2007), we investigated whether the *pgi* mutation would result in cytosolic accumulation and oxidation of DA in fly brains. HPLC analysis of DA and DOPAC levels in fly heads revealed that even at day 1 posteclosion *pgi* mutant flies possessed significantly lower DA levels (Figure S6B) and dramatically elevated DOPAC:DA ratios (Figure S6C). While  $\alpha$ -syn alone did not result in significant diminution of DA pools or elevated DA turnover at day 1, it enhanced the effects of the *pgi* mutant allele on both DA loss and DOPAC production (Fig-

ures S6B and S6C). After aging to 20 days, DA turnover in *pgi* mutants increased nearly 2.5-fold (Figure 6F). At this age,  $\alpha$ -syn flies displayed significantly reduced DA, further loss in combination with the *pgi* mutation, and an enhanced DOPAC:DA ratio (Figures 6E and 6F). These findings reveal a strong age-associated effect of *pgi* on DA regulation.

We assayed NO production in heterozygous *pgi* mutants alone and in the  $\alpha$ -syn background. Both *pgi* mutants and  $\alpha$ -syn-expressing flies individually displayed strong inflammatory responses as measured by NO production, and in combination, nearly a 4-fold increase in NO relative to control flies was observed at day 1 and day 20 posteclosion (Figures S6D and 6G). Consistent with these data, levels of the apoptosis factor DCP-1, encoded by *death caspase-1*, were significantly elevated in *pgi* mutant flies (Figure 6H). While *chico* alone showed a minor decrease in DCP-1 levels, compared to WT flies, expressing both *chico* and *pgi* together only slightly ameliorated DCP-1

protein expression triggered by the mutant *pgi* allele alone. In summary,  $\alpha$ -syn expression and *pgi* mutation individually cause deleterious effects on DA neurons, and the combination of these two modifications is synergistic in their damage to the adult *Drosophila* brain.

### Knockdown of *Gpi1*/GPI in Mouse Primary Cortical Neurons

To determine if the effect of *gpi-1/pgi* knockdown translated to a mammalian system, mouse neuronal cortical cultures were transduced with lentiviral constructs expressing a short hairpin RNA (shRNA) sequence targeted against mouse *Gpi1*. Infection of neurons at a multiplicity of infection (MOI) of 1 resulted in over 90% knockdown of GPI1 protein, compared to cells infected with a scrambled shRNA sequence (scrb), when assessed at 7 days postinfection (dpi) (Figure 7A). Neurotoxicity was determined by immunofluorescence analysis of neurofilament protein, a sensitive assay that measures the degeneration of neurites. Infection with lenti-*Gpi1*-shRNA at MOI 0.5 resulted in significant neurotoxicity compared to both non-transduced (N.T.) and scrb-infected neurons, when assessed at both 7 and 9 dpi (Figure 7B). Increasing the viral titer to an MOI of 1 further enhanced the neurotoxic effect (Figure 7C).

We subsequently characterized the effect of *Gpi1* knockdown on  $\alpha$ -syn solubility in neuronal cultures by sequential biochemical extraction. Neurons from *Gpi1*-shRNA-transduced neurons were sequentially extracted in 1% Triton X-100, 2% SDS, then 70% formic acid (FA), and compared to extracts from scrb-shRNA-infected neurons. Western blot analysis revealed that *Gpi1* knockdown significantly reduced the levels of Triton X-100-soluble monomeric  $\alpha$ -syn migrating at 18 kDa by 50%, while increasing the levels of soluble high molecular weight (HMW) oligomers by 3-fold (Figures 7D–7H). Additionally, *Gpi1* knockdown appeared to cause a dramatic accumulation of Triton X-100 insoluble  $\alpha$ -syn (~5 fold increase) extracted in SDS and FA-containing fractions (Figures 7D–7F and 7I). The solubility changes of  $\alpha$ -syn were confirmed with two antibodies that were generated against unmodified  $\alpha$ -syn (syn 202 and SNL-1), as well mAb syn 505, which was generated against oxidized/nitrated  $\alpha$ -syn (Duda et al., 2002) and recognizes cross-linked species of the protein; thus, syn 505 preferentially detects misfolded forms of  $\alpha$ -syn (Waxman et al., 2008). These results indicate that GPI1 depletion results in neurotoxicity and concomitantly causes the accumulation of soluble  $\alpha$ -syn oligomers and insoluble species.

### DISCUSSION

The wealth of information that has accumulated from decades of elegant research in model systems has led to lists of genetic factors influencing lifespan and healthspan (Kenyon, 2010; Gems and Partridge, 2013). Likewise, human genetic studies have also generated an expanding catalog of heritable and candidate susceptibility factors for PD. We set out to better define the molecular intersection of aging and PD in the context of established genetic modifiers by taking advantage of preexisting data sets and the respective strengths of select model systems. Without question, the IIS pathway is central to understanding the organ- ismal control of metabolism. We show here that reduced IIS sup-

presses  $\alpha$ -syn misfolding and neurotoxicity in flies and worms. Moreover, we identify a conserved DAF-16/FOXO-independent mechanism through which the IIS pathway integrates metabolic regulation with proteotoxicity and DA neurodegeneration.

GPI-1 is upregulated in *daf-2* mutants (Dong et al., 2007) and functions independently of DAF-16/FOXO to modulate neurodegeneration (Figure 4). Interestingly, GPI-1 RNAi/mutation extends lifespan in *C. elegans* (Schulz et al., 2007) and influences lifespan in *Drosophila* (Lai et al., 2007). While this relationship is seemingly paradoxical, it highlights the distinction between chronological aging and neuronal dysfunction and health. An expression level change in GPI-1 in *daf-2* mutant worms does not necessarily contribute to the further lifespan extension and may reflect a compensatory mechanism activated by a reduction in DAF-2 signaling. Indeed, this was implied by our result that *gpi-1 + daf-2* combinatorial RNAi abolished the protective effect of *daf-2* RNAi (Figure 5A) and was echoed by the climbing assay in flies (Figure 6A). We also determined that GPI RNAi/mutation enhances DA metabolism (Figures 6F and S6C); induces an inflammatory response and apoptosis (Figure 6G, 6H, and S6D); and causes widespread protein aggregation and neurodegeneration in worms, flies, and mammalian primary neurons (Figures 4–7; Table S2), but it does not affect ATP production (Figure S5). Furthermore, we found that increased glucose metabolism via overexpression of GPI and glucose surplus suppressed  $\alpha$ -syn-induced DA neurodegeneration in worms (Figure 4F) and flies (Figure 5F), respectively. Our data, together with Tauffenberger et al. (2012), support a role for GPI in mediating proteotoxicity and neurodegeneration via glucose metabolism.

In addition to its role as a cytoplasmic enzyme, GPI has an alternative role in cancer cells, where it acts as a ligand (GPI-1/AMF) in the AMF pathway. Its receptor, HRDL-1/AMFR, was also identified in our screen to modify  $\alpha$ -syn misfolding and neurodegeneration (Figure 4). AMF/AMFR attenuate ER stress and apoptosis in cancer cells (Fu et al., 2011). However, HRDL-1 also functions as a homolog of HRD family of E3 ligases that regulate HMG-CoA reductase degradation. The identification of HRDL-1/AMRF activity in neuroprotection suggests a potential relationship between cholesterol biosynthesis and  $\alpha$ -syn toxicity in PD. This is underscored by the results of Scherzer et al. (2003), in which changes in the expression of lipid metabolism genes represented a major response to  $\alpha$ -syn expression in *Drosophila*. Albeit (presumably) mechanistically distinct, these data are intriguing given the reported efficacy of statins in PD models (Bar-On et al., 2008). How an alteration of lipid metabolism contributes to  $\alpha$ -syn misfolding and neurotoxicity remains to be determined. Nevertheless, glucose metabolism may impact  $\alpha$ -syn toxicity through a mechanism involving the elevation of certain lipids that bind to  $\alpha$ -syn and facilitate the process of toxic oligomerization.

Importantly, three positive candidates from this study are associated with neurodegenerative disease in patients: C01A2.4/CHMP2B (frontotemporal dementia and degeneration; Isaacs et al., 2011), *gpd-2*/GAPDH (Parkinson's, Alzheimer's, and Huntington's; Mazzola and Sirover, 2001), and C54D10.10/TFPI (Alzheimer's; Piazza et al., 2012). Notably, we did not identify *C. elegans* orthologs of other known heritable PD genes among these modifiers. While this may seem surprising, in the context of reduced IIS, these findings were not completely unexpected.

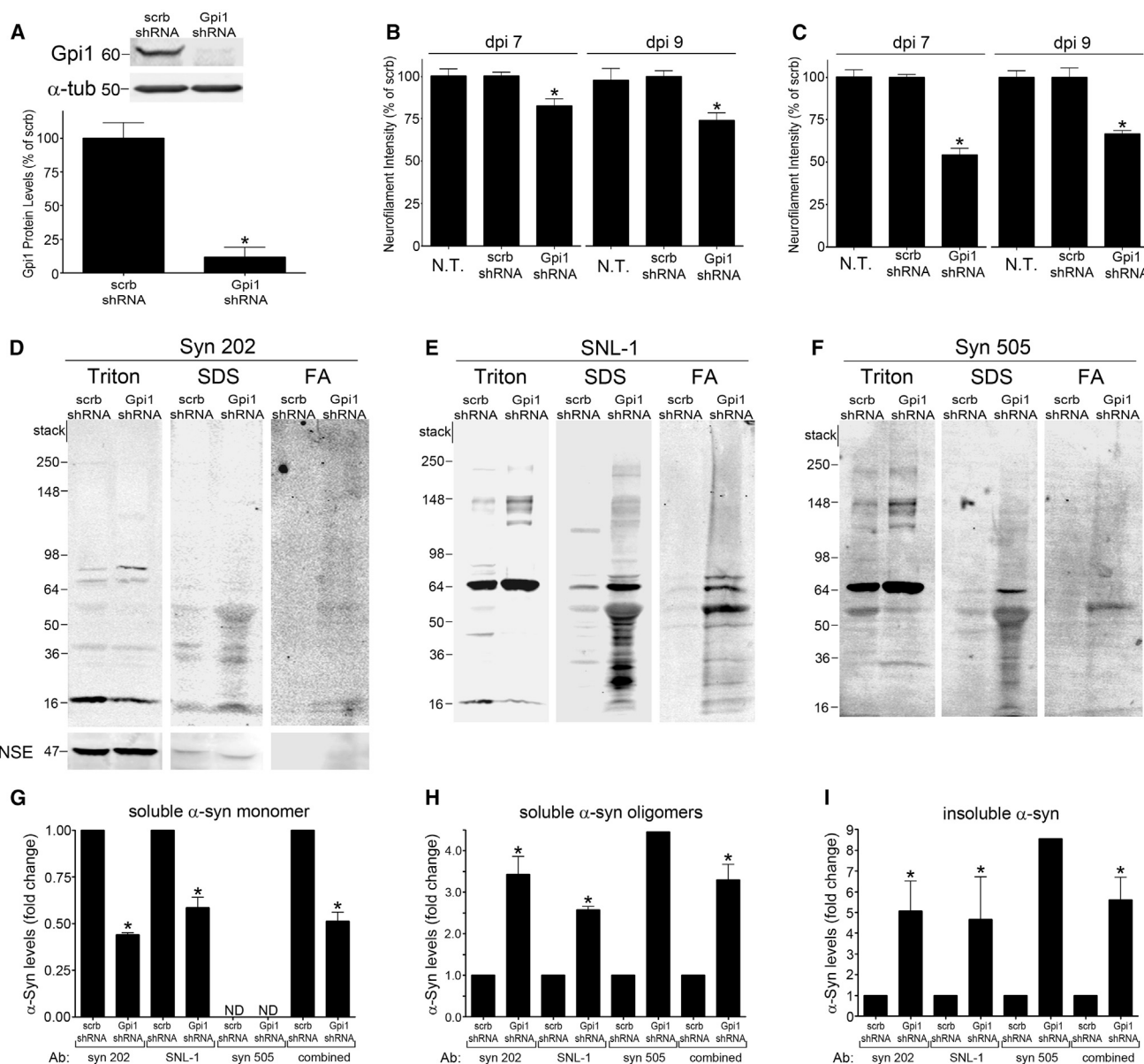


**Figure 7. Knockdown of Gpi1/GPI in Mouse Cortical Neurons Causes Neurotoxicity and  $\alpha$ -Syn Accumulation**

(A) Neurons were transduced with lenti-Gpi1 shRNA or scrambled shRNA (scrb) at MOI 1 and harvested at 7 dpi. GPI1 protein levels were determined by western blot and densitometry.  $\alpha$ -tubulin was used as a loading control (n = 4).

(B) Neurotoxicity was assessed by neurofilament measurement at dpi 7 and 9 in neurons infected at MOI 0.5.

(C) Neurotoxicity assessment at MOI 1 infection. (n = 4.)

(D–F) Sequential extraction analysis of dpi 7 neurons infected at MOI 0.5 using anti- $\alpha$ -syn antibodies syn 202, SNL-1, and syn 505. Reactivity with syn 505 reveals the presence of misfolded, oxidized/nitrated  $\alpha$ -syn. Neural specific enolase (NSE) was used as a loading control.

(G–I) Densitometric quantification of various biochemical forms of  $\alpha$ -syn (n = 2 for syn 202, n = 2 for SNL-1, and n = 1 for syn 505). Values are the mean SEM; \*p < 0.05.

Indeed, patients with monogenic forms of PD do not develop the disease until later in life, demonstrating a key role for the metabolic changes associated with aging in disease onset. Consistent with this point is the observation that energy-metabolism-associated genes are a key class of genes whose expression is modified as  $\alpha$ -syn-induced neurodegeneration progresses (Scherzer et al., 2003). Likewise, our screening paradigm involved analysis

of different phenotypes (aggregation; degeneration) in distinct cell types (bodywall muscles; dopamine neurons). Thus, contextual differences in expression may account for an absence of select modifiers. These collective results highlight the utility of model systems in deciphering the integrated consequences of imbalances in protein management and metabolic networks on neuronal survival.

## Cell Metabolism

### Metabolic Modulators OF Dopamine Neuron Loss

CellPress

#### EXPERIMENTAL PROCEDURES

##### Basic *C. elegans* Genetic and Biochemical Methods

Strain maintenance, genetic crosses, creation of transgenic nematodes, and supporting biochemical procedures were carried out using standard methods (see [Supplemental Experimental Procedures](#) for details).

##### *C. elegans* RNAi Screening

Screening was performed using RNAi feeding clones (Geneservice, Cambridge). Twenty age-synchronized young adult F1 animals were analyzed per clone. The RNAi clones resulting in significant  $\alpha$ -syn aggregation (80% of worms with increased quantity and size of aggregates) were scored as positive, and all positives were tested in triplicate. RNAi feeding procedures, assays, and worm strains are described in the [Supplemental Experimental Procedures](#).

##### *C. elegans* Secondary Screening of Candidate Genes from RNAi Screen

Nematode models of polyglutamine aggregation in bodywall muscle cells, A $\beta$  paralysis, DAF-16::GFP localization, and  $\alpha$ -syn-induced DA neurodegeneration were examined as secondary screening assays. These models were interrogated using RNAi of the 60 gene candidates identified from the screen by exploring by the impact of gene knockdown on F1 offspring (versus EV RNAi). Polyglutamine aggregation and A $\beta$  paralysis worm models (*daf-2*; *P<sub>unc-54</sub>::Q82::GFP* and *P<sub>myo-3</sub>::A $\beta$ <sub>1-42</sub>*) were scored at the L3-stage for total number of aggregates or numbers of worms paralyzed, respectively. DA neurons were also examined for  $\alpha$ -syn-induced neurodegeneration in 7-day-old animals (*sid-1*; *P<sub>unc-119</sub>::sid-1*; *P<sub>daf-1</sub>:: $\alpha$ -syn*; *P<sub>daf-1</sub>::GFP*) that had been exposed to RNAi since embryonic stages. A worm was considered rescued when all six anterior DA neurons were intact had no visible signs of degeneration. Statistical analyses for RNAi experiments with Q82 aggregation, A $\beta$  paralysis, and DA neuron degeneration were performed using the one-way ANOVA with Dunnett's post hoc test ( $p < 0.05$ ) to compare control worms (fed RNAi bacteria not targeting any gene) with experimental worms (fed RNAi bacteria targeting candidate gene). *C. elegans* scored for DAF-16::GFP localization were L3 staged and had been exposed to RNAi since the embryonic stage (*daf-2*; *P<sub>daf-16a/b</sub>::GFP*). For each worm, GFP localization was scored as "completely nuclear," "both nuclear and cytoplasmic," or "completely cytoplasmic." Two independent trials ( $n = 40$  total) were performed, and positives were determined as significant if  $p < 0.05$ , via a chi-square test. [Supplemental Experimental Procedures](#) provide more details for all of these procedures.

##### *C. elegans* ts Mutant Phenotype Assays

The nematode mutants, *unc-15* and *unc-52*, were treated with EV or *gpi-1* RNAi and maintained at permissive temperature. Behavioral analysis was recorded and analyzed using WormLab3.0 (MBF Bioscience) with Kalman smoothing. Three independent trials were conducted, each with 15–20 worms. An unpaired Student's two-tailed t test with Welch correction was used to determine statistical significance (see [Supplemental Experimental Procedures](#) for details).

##### DOG Analysis in *C. elegans*

DA neurodegeneration assays were performed on *P<sub>daf-1</sub>:: $\alpha$ -syn*, *P<sub>daf-1</sub>::GFP* animals that were age-synchronized, exposed to 5 or 10 mM DOG for 24 hr, and analyzed at day 4. Three trials were performed ( $n = 90$  animals/treatment); one-way ANOVA with Dunnett post hoc test.

##### Ingenuity Pathway Analysis

The Ingenuity Pathway Analysis (IPA) software (Ingenuity® Systems; <http://www.ingenuity.com>) was used for distributing the 60 positive candidate genes from our primary screen into biological networks and for evaluation of functional significance.

##### Basic *Drosophila* Genetic and Biochemical Methods

Strain maintenance, genetic crosses, and supporting biochemical procedures were carried out using standard methods (see [Supplemental Experimental Procedures](#) for details).

##### *Drosophila* DA Neuron Quantification

DA neurons from adult males were dissected for analysis either 1 or 20 days posteclosion. These neurons were visualized by expression of GFP under the control of the DA neuron driver TH-Gal4, and samples were quantified following confocal microscopy imaging. Additional details are outlined in the [Supplemental Experimental Procedures](#) section.

##### *Drosophila* DA Neuron HPLC and NO Synthase Analyses

Monoamines from male heads were separated using HPLC as described in Chaudhuri et al. (2007). A modified Griess reagent assay described in Ajjuri and O'Donnell (2013) was used to quantify nitric oxide synthase activity. Male heads were also examined in this assay. For all experiments, genotypes were analyzed in triplicate and statistics were analyzed using one-way ANOVA followed by Dunnett post hoc test. See [Supplemental Experimental Procedures](#) for more details.

##### *Drosophila* DOG and Glucose Feeding

Male flies were aged to 10 days posteclosion and then fed either standard corn syrup food or standard food supplemented with either 200 mM 2-DOG or glucose with a final concentration of 1 M continuously for 5 days. Statistics were analyzed using one-way ANOVA followed by Bonferroni post hoc test.

##### *Drosophila* Climbing Assay

Flies were anesthetized using cold coma, transferred in groups of ten to climbing vials, and allowed 45 min to recuperate. Vials were gently tapped before each trial, and climbing was scored by calculating the number of flies to climb 6 cm in 20 s. The results represent ten trials with three repetitions per trial. Statistical analyses were performed using one-way ANOVA with Bonferroni post hoc test.

##### Mouse Cortical Cultures, Lentiviral Infection, and Neurotoxicity Analysis

Murine neuronal cortical cells were obtained at embryonic day 17, as previously described (Tsika et al., 2010). Cells were seeded in 96-well plates at 50,000 cells/well and infected at 5 days in vitro (DIV) with lentiviral particles containing shRNA against *Gpi1* at either MOI 0.5 or 1. The cells were then fixed in 4% paraformaldehyde at the indicated time points. The staining and analysis procedures have been described in detail previously (Tsika et al., 2010). Neurotoxicity analysis was performed with two separate culture preparations, with four replicates for each preparation. One-way ANOVA with Tukey's post hoc test was used to determine statistical significance, and  $p < 0.05$  was considered significant. See [Supplemental Experimental Procedures](#) for details.

##### Sequential Biochemical Extraction of Mouse Neuronal Cultures

6,000,000 cells/condition were extracted for SDS-PAGE analyses using the methods described in the [Supplemental Experimental Procedures](#) section. The subsequent gels were transferred to polyvinylidene difluoride membranes and probed with anti- $\alpha$ -syn antibodies (syn 202, dilution 1:500; Covance; SNL-1, dilution 1:500, gift of Benoit I. Giasson, University of Pennsylvania; or syn 505, dilution 1:500, Invitrogen). Anti-Neural-specific enolase and anti-alpha-tubulin were used as loading controls. Primary antibodies were detected with anti-mouse or rabbit IgG conjugated to IRDye 680 or 800. For controls, blots were scanned after the blocking step to determine autofluorescent bands and also after the addition of secondary Ab alone. Any nonspecific bands detected were not included in densitometric analyses. Quantification of the Triton-soluble band migrating at 18 kDa was used for monomer measurements (syn 202 and SNL-1); quantification of aggregated forms of  $\alpha$ -syn was done with syn 202, SNL-1, and syn 505 and repeated with separated culture preparations. A Student's t test was used to determine statistical significance;  $p < 0.05$  was considered significant.

#### SUPPLEMENTAL INFORMATION

Supplemental Information includes six figures, three tables, three movies, and Supplemental Experimental Procedures and can be found with this article online at <http://dx.doi.org/10.1016/j.cmet.2014.04.017>.

## ACKNOWLEDGMENTS

We are grateful to all members of the Caldwell and O'Donnell labs for their collegiality and collective teamwork. Special thanks to Laura Berkowitz for her invaluable contributions and Chris Link and Richard Morimoto for the A $\beta$  paralysis and Q82::GFP strains, respectively. Some strains were provided by the CGC, which is funded by NIH Office of Research Infrastructure Programs (P40 OD010440). This research was funded by grants from the National Institutes of Health (R15 NS075684-01 to G.A.C. and R15 NS078728 to J.M.O.). Other support came from a Howard Hughes Medical Institute Undergraduate Science Program Grant to The University of Alabama (A.R.B., S.K.L., and S.M.D.), as well as the Parkinson's Support Group of Huntsville (L.R.R.) and the Parkinson's Association of Alabama (A.L.K. and M.W.Z.).

Received: October 29, 2013

Revised: March 16, 2014

Accepted: April 17, 2014

Published: May 29, 2014

## REFERENCES

- Ajjuri, R.R., and O'Donnell, J.M. (2013). Novel whole-tissue quantitative assay of nitric oxide levels in *Drosophila* neuroinflammatory response. *J. Vis. Exp.* 82, 50892, <http://dx.doi.org/10.3791/50892>.
- Amaducci, L., and Tesco, G. (1994). Aging as a major risk for degenerative diseases of the central nervous system. *Curr. Opin. Neurol.* 7, 283–286.
- Bar-On, P., Crews, L., Koob, A.O., Mizuno, H., Adame, A., Spencer, B., and Masliah, E. (2008). Statins reduce neuronal alpha-synuclein aggregation in vitro models of Parkinson's disease. *J. Neurochem.* 105, 1656–1667.
- Bocchitto, M., Lamitina, T., and Kalb, R.G. (2012). Daf-2 signaling modifies mutant SOD1 toxicity in *C. elegans*. *PLoS ONE* 7, e33494.
- Cao, S., Gelwix, C.C., Caldwell, K.A., and Caldwell, G.A. (2005). Torsin-mediated protection from cellular stress in the dopaminergic neurons of *Caenorhabditis elegans*. *J. Neurosci.* 25, 3801–3812.
- Chaudhuri, A., Bowling, K., Funderburk, C., Lawal, H., Inamdar, A., Wang, Z., and O'Donnell, J.M. (2007). Interaction of genetic and environmental factors in a *Drosophila* parkinsonism model. *J. Neurosci.* 27, 2457–2467.
- Clancy, D.J., Gems, D., Harshman, L.G., Oldham, S., Stocker, H., Hafen, E., Leivers, S.J., and Partridge, L. (2001). Extension of life-span by loss of CHICO, a *Drosophila* insulin receptor substrate protein. *Science* 292, 104–106.
- Cohen, E., and Dillin, A. (2008). The insulin paradox: aging, proteotoxicity and neurodegeneration. *Nat. Rev. Neurosci.* 9, 759–767.
- Cohen, E., Bieschke, J., Perciavalle, R.M., Kelly, J.W., and Dillin, A. (2006). Opposing activities protect against age-onset proteotoxicity. *Science* 313, 1604–1610.
- Dong, M.Q., Venable, J.D., Au, N., Xu, T., Park, S.K., Cociorva, D., Johnson, J.R., Dillin, A., and Yates, J.R., 3rd. (2007). Quantitative mass spectrometry identifies insulin signaling targets in *C. elegans*. *Science* 317, 660–663.
- Dostal, V., and Link, C.D. (2010). Assaying  $\beta$ -amyloid toxicity using a transgenic *C. elegans* model. *J. Vis. Exp.* 44, e2252, <http://dx.doi.org/10.3791/2252>.
- Duda, J.E., Giasson, B.I., Mabon, M.E., Lee, V.M.-Y., and Trojanowski, J.Q. (2002). Novel antibodies to synuclein show abundant striatal pathology in Lewy body diseases. *Ann. Neurol.* 52, 205–210.
- Fu, M., Li, L., Albrecht, T., Johnson, J.D., Kojic, L.D., and Nabi, I.R. (2011). Autocrine motility factor/phosphoglucose isomerase regulates ER stress and cell death through control of ER calcium release. *Cell Death Differ.* 18, 1057–1070.
- Gems, D., and Partridge, L. (2013). Genetics of longevity in model organisms: debates and paradigm shifts. *Annu. Rev. Physiol.* 75, 621–644.
- Gidalevitz, T., Ben-Zvi, A., Ho, K.H., Brignull, H.R., and Morimoto, R.I. (2006). Progressive disruption of cellular protein folding in models of polyglutamine diseases. *Science* 311, 1471–1474.
- Haga, A., Niinaka, Y., and Raz, A. (2000). Phosphohexose isomerase/autocrine motility factor/neuroleukin/maturation factor is a multifunctional phosphoprotein. *Biochim. Biophys. Acta* 1480, 235–244.
- Halaschek-Wiener, J., Khattra, J.S., McKay, S., Pouzyrev, A., Stott, J.M., Yang, G.S., Holt, R.A., Jones, S.J.M., Marra, M.A., Brooks-Wilson, A.R., and Riddle, D.L. (2005). Analysis of long-lived *C. elegans* daf-2 mutants using serial analysis of gene expression. *Genome Res.* 15, 603–615.
- Hamamichi, S., Rivas, R.N., Knight, A.L., Cao, S., Caldwell, K.A., and Caldwell, G.A. (2008). Hypothesis-based RNAi screening identifies neuroprotective genes in a Parkinson's disease model. *Proc. Natl. Acad. Sci. USA* 105, 728–733.
- Harrington, A.J., Yacoubian, T.A., Slone, S.R., Caldwell, K.A., and Caldwell, G.A. (2012). Functional analysis of VPS41-mediated neuroprotection in *Caenorhabditis elegans* and mammalian models of Parkinson's disease. *J. Neurosci.* 32, 2142–2153.
- Isaacs, A.M., Johannsen, P., Holm, I., and Nielsen, J.E.; FR $\alpha$ J Consortium (2011). Frontotemporal dementia caused by CHMP2B mutations. *Curr. Alzheimer Res.* 8, 246–251.
- Kenyon, C.J. (2010). The genetics of ageing. *Nature* 464, 504–512.
- Kuwahara, T., Koyama, A., Koyama, S., Yoshina, S., Ren, C.H., Kato, T., Mitani, S., and Iwatsubo, T. (2008). A systematic RNAi screen reveals involvement of endocytic pathway in neuronal dysfunction in  $\alpha$ -synuclein transgenic *C. elegans*. *Hum. Mol. Genet.* 17, 2997–3009.
- Lai, C.-Q., Parnell, L.D., Lyman, R.F., Ordovas, J.M., and Mackay, T.F.C. (2007). Candidate genes affecting *Drosophila* life span identified by integrating microarray gene expression analysis and QTL mapping. *Mech. Ageing Dev.* 128, 237–249.
- Lin, K., Hsin, H., Libina, N., and Kenyon, C. (2001). Regulation of the *Caenorhabditis elegans* longevity protein DAF-16 by insulin/IGF-1 and germline signaling. *Nat. Genet.* 28, 139–145.
- Mazzola, J.L., and Sirover, M.A. (2001). Reduction of glyceraldehyde-3-phosphate dehydrogenase activity in Alzheimer's disease and in Huntington's disease fibroblasts. *J. Neurochem.* 76, 442–449.
- McElwee, J.J., Schuster, E., Blanc, E., Thomas, J.H., and Gems, D. (2004). Shared transcriptional signature in *Caenorhabditis elegans* Dauer larvae and long-lived daf-2 mutants implicates detoxification system in longevity assurance. *J. Biol. Chem.* 279, 44533–44543.
- Morley, J.F., Brignull, H.R., Weyers, J.J., and Morimoto, R.I. (2002). The threshold for polyglutamine-expansion protein aggregation and cellular toxicity is dynamic and influenced by aging in *Caenorhabditis elegans*. *Proc. Natl. Acad. Sci. USA* 99, 10417–10422.
- Murphy, C.T., McCarroll, S.A., Bargmann, C.I., Fraser, A., Kamath, R.S., Ahringer, J., Li, H., and Kenyon, C. (2003). Genes that act downstream of DAF-16 to influence the lifespan of *Caenorhabditis elegans*. *Nature* 424, 277–283.
- Nollen, E.A.A., Garcia, S.M., van Haaften, G., Kim, S., Chavez, A., Morimoto, R.I., and Plasterk, R.H.A. (2004). Genome-wide RNA interference screen identifies previously undescribed regulators of polyglutamine aggregation. *Proc. Natl. Acad. Sci. USA* 101, 6403–6408.
- Piazza, F., Galimberti, G., Conti, E., Isella, V., Perlangeli, M.V., Speranza, T., Borroni, B., Pogliani, E.M., Padovani, A., and Ferrarese, C. (2012). Increased tissue factor pathway inhibitor and homocysteine in Alzheimer's disease. *Neurobiol. Aging* 33, 226–233.
- Robida-Stubbs, S., Glover-Cutter, K., Lamming, D.W., Mizunuma, M., Narasimhan, S.D., Neumann-Haefelin, E., Sabatini, D.M., and Blackwell, T.K. (2012). TOR signaling and rapamycin influence longevity by regulating SKN-1/Nrf and DAF-16/FoxO. *Cell Metab.* 15, 713–724.
- Samuelson, A.V., Carr, C.E., and Ruvkun, G. (2007). Gene activities that mediate increased life span of *C. elegans* insulin-like signaling mutants. *Genes Dev.* 21, 2976–2994.
- Scherzer, C.R., Jensen, R.V., Gullans, S.R., and Feany, M.B. (2003). Gene expression changes presage neurodegeneration in a *Drosophila* model of Parkinson's disease. *Hum. Mol. Genet.* 12, 2457–2466.

- Schulz, T.J., Zarse, K., Voigt, A., Urban, N., Birringer, M., and Ristow, M. (2007). Glucose restriction extends *Caenorhabditis elegans* life span by inducing mitochondrial respiration and increasing oxidative stress. *Cell Metab.* 6, 280–293.
- Suh, Y., Atzmon, G., Cho, M.-O., Hwang, D., Liu, B., Leahy, D.J., Barzilai, N., and Cohen, P. (2008). Functionally significant insulin-like growth factor I receptor mutations in centenarians. *Proc. Natl. Acad. Sci. USA* 105, 3438–3442.
- Taguchi, A., and White, M.F. (2008). Insulin-like signaling, nutrient homeostasis, and life span. *Annu. Rev. Physiol.* 70, 191–212.
- Tatar, M., Kopelman, A., Epstein, D., Tu, M.-P., Yin, C.-M., and Garofalo, R.S. (2001). A mutant *Drosophila* insulin receptor homolog that extends life-span and impairs neuroendocrine function. *Science* 292, 107–110.
- Tauffmanberger, A., Vaccaro, A., Aulas, A., Vande Velde, C., and Parker, J.A. (2012). Glucose delays age-dependent proteotoxicity. *Aging Cell* 11, 856–866.
- Tsika, E., Moysidou, M., Guo, J., Cushman, M., Gannon, P., Sandaltzopoulos, R., Giasson, B.I., Krainc, D., Ischiropoulos, H., and Mazzulli, J.R. (2010). Distinct region-specific  $\alpha$ -synuclein oligomers in A53T transgenic mice: implications for neurodegeneration. *J. Neurosci.* 30, 3409–3418.
- Tsuda, M., Kobayashi, T., Matsuo, T., and Aigaki, T. (2010). Insulin-degrading enzyme antagonizes insulin-dependent tissue growth and A $\beta$ -induced neurotoxicity in *Drosophila*. *FEBS Lett.* 584, 2916–2920.
- van Ham, T.J., Thijssen, K.L., Breitling, R., Hofstra, R.M.W., Plasterk, R.H.A., and Nollen, E.A.A. (2008). *C. elegans* model identifies genetic modifiers of  $\alpha$ -synuclein inclusion formation during aging. *PLoS Genet.* 4, e1000027.
- Vartiainen, S., Pehkonen, P., Lakso, M., Nass, R., and Wong, G. (2006). Identification of gene expression changes in transgenic *C. elegans* overexpressing human  $\alpha$ -synuclein. *Neurobiol. Dis.* 22, 477–486.
- Waxman, E.A., Duda, J.E., and Giasson, B.I. (2008). Characterization of antibodies that selectively detect alpha-synuclein in pathological inclusions. *Acta Neuropathol.* 116, 37–46.
- Yamamoto, R., and Tatar, M. (2011). Insulin receptor substrate *chico* acts with the transcription factor FOXO to extend *Drosophila* lifespan. *Aging Cell* 10, 729–732.